Modeling the chemistry of ozone, halogen compounds, and hydrocarbons in the arctic troposphere during spring

By ROLF SANDER[1]*, RAINER VOGT[2,3], GEOFF W. HARRIS[1] and PAUL J. CRUTZEN[2],

ABSTRACT

The box model MoccaIce has been developed to study the chemistry of the arctic boundary layer. It treats chemical reactions in the gas phase and in the aerosol, as well as exchange between the 2 phases. Photolysis rates vary according to the solar declination during polar sunrise. Apart from the standard tropospheric chemistry of ozone, hydrocarbons, and nitrogen species, the reaction mechanism includes sulfur and the halogens Cl, Br, and I. Modeling an ozone depletion event, we found that iodine species contribute to the chemical destruction of ozone significantly if IO mixing ratios are about 1 pmol/mol. The reactions of BrO with BrO and IO are the main pathways of the ozone destruction cycle. Hydrocarbon concentrations decrease during ozone depletion events due to reaction with halogen atoms. The rate of ozone destruction depends on whether the addition of Br to C_2H_4 and C_2H_2 yields inert products or intermediates from which Br can be regenerated. Bromine and HCHO are positively correlated. The model produces HCHO during ozone depletion events, though not as much as reported from field observations. After the destruction of ozone has been competed, the halogen species are converted to halides and subsequently scavenged by aerosol particles.

1. Introduction

Results of polar sunrise observations in the Arctic have revealed an annual increase of particulate bromine in the spring (Berg et al., 1983). At the same time of year, low concentrations of ozone were observed (Oltmans & Komhyr, 1986). It has been suggested by Barrie et al. (1988) that the destruction of ozone is mainly due to catalytic reactions of bromine species. There is now evidence of the presence of BrO radicals from field measurements (Hausmann & Platt, 1994). During the ozone depletion events, mixing ratios of alkanes, alkenes and alkynes decrease (Jobson et al., 1994) while HCHO increases (de Serves, 1994). This is consistent with the assumption that reactive chlorine as well as bromine is present in the arctic troposphere. In addition, during measurements in Spitzbergen a tentative detection of tropospheric IO was made (Unold et al., 1996). Particulate iodine was found to be at concentrations around 1 ng/m^3 in accumulation mode aerosols (Barrie et al., 1994). It has been suggested that iodine also contributes significantly to the destruction of tropospheric ozone (Chameides and Davis, 1980; Wayne et al., 1995; Davis et al., 1996). However, no detailed model calculations of arctic ozone depletion events were made.

In this paper, we use a box model to investigate halogen chemistry and ozone depletion in the polar boundary layer during arctic spring. Results of model calculations are presented to illustrate the contributions of chlorine, bromine and iodine

to ozone depletion, hydrocarbon oxidation and HCHO formation.

2. Model description

The box model MoccaIce (Model Of Chemistry Considering Aerosols In Cold Environments) has been developed to study the chemistry of the arctic boundary layer. Previously used to model the chemistry in marine air at mid-latitudes (Sander & Crutzen, 1996; Vogt et al., 1996), it has now been modified to describe polar sunrise chemistry in the Arctic. A total of 82 gas-phase and 68 aqueous-phase species are included. The model treats gas-phase chemical reactions and reactions in the deliquesced sulfate particles, as well as exchange between the 2 phases. Recently, modules containing chemical mechanisms for non-methane hydrocarbons (NMHC's) and iodine species have been added to the original model. It now contains 145 gas-phase reactions, 45 photolysis reactions, 45 phase transfer processes, and 102 aqueous-phase reactions.

2.1. *Adaptation to polar sunrise conditions and model initialization*

Temperature and relative humidity were set to $T = 240$ K and $\varphi_v = 80\%$, respectively. The solar elevation angle is obtained by applying the equations given by Stull (1988) to a latitude of 82°N. Photolysis rates of iodine species were calculated by C. Brühl (personal communication) using the model described by Brühl & Crutzen (1989) and uv/vis spectra from several sources (Roehl et al., 1997; Laszlo et al., 1995; Tellinghuisen, 1973; Seery & Britton, 1964). Other photolysis rates were calculated as a function of the solar elevation angle by T. Tang (personal communication) using the model described by Henderson et al. (1987). Deposition velocities and entrainment of ozone from the free troposphere were set to zero, since the arctic boundary layer is very stable during ozone depletion events and deposition on ice is very slow.

Model runs were performed starting on Julian day (JD) 90 and lasting 10 days (i.e. 1–10 April). Table 1 lists the initial gas-phase mixing ratios which were approximately set to values encountered in arctic air masses in the spring (Worthy et al., 1994,; Jobson et al., 1994; Muthuramu et al., 1994; de Serves, 1994; Heidt et al., 1980; Yokouchi et al., 1994). To simulate an ozone depletion event caused by a (so far unidentified) marine halogen source, emissions of Br_2 and Cl_2 were switched on from JD 94 until JD 97 at rates of 17 pmol mol^{-1} day^{-1} and 113 pmol mol^{-1} day^{-1}, respectively. These rates were chosen in order to destroy ozone within 3 days and to match the observed decay of hydrocarbons.

2.2. *Aerosol parametrization and chemistry*

The aerosol module of MoccaIce was adapted to arctic sulfate particles in the accumulation mode. Sea-salt particles are not considered in the current model version because of their lower concentration. Staebler et al. (1994) found that sulfate particles contribute 95% of the total surface available for heterogeneous reactions. We use a lognormal size distribution based on their measurements:

$$\frac{\mathrm{d}^1N}{\mathrm{d}\lg r} = \frac{n}{\lg\sigma\sqrt{2\pi}} \times \exp\left(-\frac{(\lg r - \lg R)^2}{2(\lg\sigma)^2}\right), \quad (1)$$

where ^1N is the number of aerosol particles per volume with radius less than r, r is radius, $n = 280$ cm^{-3} is the number density, $R = 0.1$ μm is the mean droplet radius, and $\lg\sigma = 0.17$ is the decadic logarithm of the standard deviation from R. Integration over the entire size range yields a liquid water content of $L = 2 \times 10^{-12}$ m^3(aq)/m^3(air). The particles contain 37 mass-% sulfate in order to be in equilibrium with ambient air according to the Köhler equation (Pruppacher & Klett, 1978).

The aqueous-phase chemistry of the aerosol particles focuses on the transformation of halides into more reactive forms. Important reactions producing Br_2 and BrCl were suggested by Fan & Jacob (1992) and Vogt et al. (1996):

$$HOBr + Br^- + H^+ \rightleftharpoons Br_2 + H_2O, \quad (2)$$

$$HOBr + Cl^- + H^+ \rightleftharpoons BrCl + H_2O. \quad (3)$$

We have also included the permutations of the analogous reactions:

$$HOX + Y^- + H^+ \rightleftharpoons XY + H_2O, \quad (4)$$

with X, Y = Cl, Br, or I. Their rate constants are listed in Table 2. The interhalogen compounds XY produced here are in equilibrium with chloride

Table 1. *Initial gas-phase mixing ratios*

O_3	=	30 nmol/mol	C_2H_6	=	2.5 nmol/mol	C_2H_4	= 100 pmol/mol
NO_x	=	20 pmol/mol	C_3H_8	=	1.6 nmol/mol	C_2H_2	= 800 pmol/mol
$RONO_2$	=	140 pmol/mol	n-C_4H_{10}	=	400 pmol/mol	C_6H_6	= 200 pmol/mol
CH_4	=	1800 nmol/mol	iso-C_4H_{10}	=	300 pmol/mol	CH_3Br	= 5.0 pmol/mol
HCHO	=	50 pmol/mol	n-C_5H_{12}	=	200 pmol/mol	$CHBr_3$	= 3.5 pmol/mol
CO	=	170 nmol/mol	iso-C_5H_{12}	=	200 pmol/mol	CH_3I	= 2 pmol/mol

Table 2. *Aqueous-phase rate constants for the reactions* $HOX + Y^- + H^+ \rightleftharpoons XY + H_2O$

Reaction (of order n)	n	k / $M^{1-n}s^{-1}$	Ref.
$HOCl + Cl^- + H^+ \rightarrow Cl_2 + H_2O$	3	2.2×10^4	Wang & Margerum [1994]
$HOCl + Br^- + H^+ \rightarrow BrCl + H_2O$	3	1.3×10^6	Kumar & Margerum [1987]
$HOCl + I^- + H^+ \rightarrow ICl + H_2O$	3	3.5×10^{11}	Nagy et al. [1988]
$HOBr + Cl^- + H^+ \rightarrow BrCl + H_2O$	3	5.6×10^9	Wang et al. [1994][a]
$HOBr + Br^- + H^+ \rightarrow Br_2 + H_2O$	3	1.6×10^{10}	Beckwith et al. [1996][a]
$HOBr + I^- \rightarrow IBr + OH^-$	2	5.0×10^9	Troy & Margerum [1991]
$HOI + Cl^- + H^+ \rightarrow ICl + H_2O$	3	2.9×10^{10}	Wang et al. [1989][a]
$HOI + Br^- + H^+ \rightarrow IBr + H_2O$	3	3.3×10^{12}	Troy et al. [1991][a]
$HOI + I^- + H^+ \rightarrow I_2 + H_2O$	3	4.4×10^{12}	Eigen & Kustin [1962]
$Cl_2 \rightarrow HOCl + Cl^- + H^+$	1	2.2×10^1	Wang & Margerum [1994]
$Br_2 \rightarrow HOBr + Br^- + H^+$	1	9.7×10^1	Beckwith et al. [1996]
$BrCl \rightarrow HOBr + Cl^- + H^+$	1	1.0×10^5	Wang et al. [1994]
$ICl \rightarrow HOI + Cl^- + H^+$	1	2.4×10^6	Wang et al. [1989]
$IBr \rightarrow HOI + Br^- + H^+$	1	8.0×10^5	Troy et al. [1991]

[a] Calculated from equilibrium and back reaction.

and bromide (Wang et al., 1994), e.g.:

$$BrCl + Br^- \rightleftharpoons Br_2 + Cl^-. \quad (5)$$

Due to their low solubility, the halogens and interhalogen componds volatilize quickly into the gas phase.

2.3. *The chemistry of non-methane hydrocarbons*

In order to compare experimentally observed values for several organic species with model results, the chemical mechanism of MoccaIce has been extended to include a non-methane hydrocarbon module. The very complex organic chemistry is treated in a simplified way which does not attempt to resolve secondary reactions of peroxy radicals and other intermediates. However, the reaction scheme was chosen such that the decay of the primary hydrocarbons, the production of HCHO, and the mass balance of bromine, are described properly. Species included explicitly are: C_2H_6, C_3H_8, *n*-C_4H_{10}, iso-C_4H_{10}, *n*-C_5H_{12}, iso-C_5H_{12}, C_2H_4, C_2H_2, C_6H_6, C_2HCl_3, C_2Cl_4, CH_3Br, $CHBr_3$, CH_3I, C_3H_7I, CH_2ClI, and CH_2I_2.

Alkanes react with OH and Cl. Hydrogen abstraction and subsequent addition of oxygen leads to the formation of peroxy radicals. To simplify the complex nature of secondary reactions, all alkanes produce a generic radical RCH_2OO in the model. The only exception is CH_3OO, which is treated explicitly. Ethene and ethyne react with OH, Cl and Br. Although there have been investigations of the Br-initiated reactions (Banes et al., 1989; Yarwood et al., 1991), the distribution of products is not exactly known. In the model we include:

$$C_2H_2 + Br \xrightarrow{O_2} BrCHO + CO + HO_2 \quad (6)$$

$$\xrightarrow{O_2} Br(+OHCCHO), \quad (7)$$

with a 15% yield of BrCHO. The fate of OHCCHO is not considered further. Major products of the reaction $C_2H_4 + Br$ are $BrCH_2CHO$, $BrCH_2CH_2OH$, and $BrCH_2CH_2OOH$ (Yarwood et al., 1992). For simplification, we define R'Br in the model representing a generic Br-containing intermediate resulting from the addition of Br to a C–C multiple bond. We assume that R'Br hydrolyzes to HBr on aerosol particles and estimate an accommodation coefficient of $\alpha = 0.1$.

Secondary reactions include the self-reaction of the peroxy radicals and their reactions with HO_2 and NO:

$$RCH_2OO + RCH_2OO \rightarrow 2RCH_2O + O_2, \quad (8)$$

$$RCH_2OO + HO_2 \rightarrow RCH_2OOH + O_2, \quad (9)$$

$$RCH_2OO + NO \rightarrow RCH_2O + NO_2. \quad (10)$$

There are two pathways for the reaction of alkoxy radicals RCH_2O in the presence of oxygen:

$$RCH_2O + O_2 \rightarrow HCHO + RO_2 \quad (11)$$

$$\rightarrow RCHO + HO_2. \quad (12)$$

In the case of R = H, both channels are identical and produce HCHO. This is in fact the main HCHO production path. If $R \neq H$, we assume a 1% probability for the first channel. The aldehyde RCHO produced in the 2nd channel also eventually contributes to the formation of HCHO:

$$RCHO + OH/Cl/Br \rightarrow R + CO + H_2O/HCl/HBr \quad (13)$$

$$R + O_2 \rightarrow RO_2. \quad (14)$$

This yields another peroxy radical (with one C atom less) which in turn reacts as described above. Since in our parametrization we do not have different peroxy radicals, we assume that reaction (14) produces CH_3OO.

2.4. *Iodine chemistry*

The iodine chemistry module is based on reaction schemes described by Chameides & Davis (1980), Chatfield & Crutzen (1990), and Jenkin (1992). In addition, photolysis of the iodocarbons CH_2I_2, CH_2ClI, and C_3H_7I has been included in the model. Recently, these compounds have been detected in ocean water (Moore & Tokarczyk, 1992; Klick & Abrahamson, 1992) and in the arctic atmosphere (Schall & Heumann, 1993). We assume emission rates of 0.6 pmol mol^{-1} day^{-1} for CH_3I and C_3H_7I, and 1.2 pmol mol^{-1} day^{-1} for CH_2I_2 and CH_2ClI from JD 94 until JD 97. These values were chosen such that the total organic iodine mixing ratio is about 3 pmol/mol, consistent with observations by Schall & Heumann (1993).

The gas-phase reaction scheme includes the reactions IO + ClO, IO + BrO, and I + BrO with rate constants taken from Turnipseed et al. (1995) and Laszlo et al. (1996). In the model, scavenging of inorganic iodine compounds (HOI, IO, HI, INO_3, INO_2, I_2O_2, I_2, ICl, and IBr) by the sulfate aerosol is considered. However, unlike earlier iodine models, aqueous-phase reactions are also included. For example, HOI scavenged by the aerosol reacts with the halide ions Cl^-, Br^-, or I^- (Table 2). The resulting interhalogen compounds ICl and IBr, as well as molecular iodine, are only slightly soluble and volatilize rapidly. Scavenging of I_2O_2 and subsequent hydrolysis yields HOI and IO_2^-, which in turn can be oxidized by H_2O_2 to iodate:

$$I_2O_2 + H_2O \rightarrow HOI + H^+ + IO_2^- \quad (15)$$

$$IO_2^- + H_2O_2 \rightarrow IO_3^- + H_2O. \quad (16)$$

Oxidation to iodate is irreversible and therefore this species accumulates in the aerosol.

3. Results and discussion

3.1. *Ozone destruction*

The gas-phase mixing ratios of O_3, OH, and HO_2 in the base run of the model are shown in Fig. 1 (solid line). Ozone remains constant until JD 94. The only source of bromine in that period is photolysis of $CHBr_3$ which is too small to be significant. After switching on the halogen emissions, ozone is completely destroyed within 3 days. Most of the ozone is destroyed by reactions involving bromine radicals. Br atoms are oxidized by ozone to BrO. A large portion of BrO is photolyzed back to Br and O. Since O quickly adds to molecular oxygen, there is no net effect of

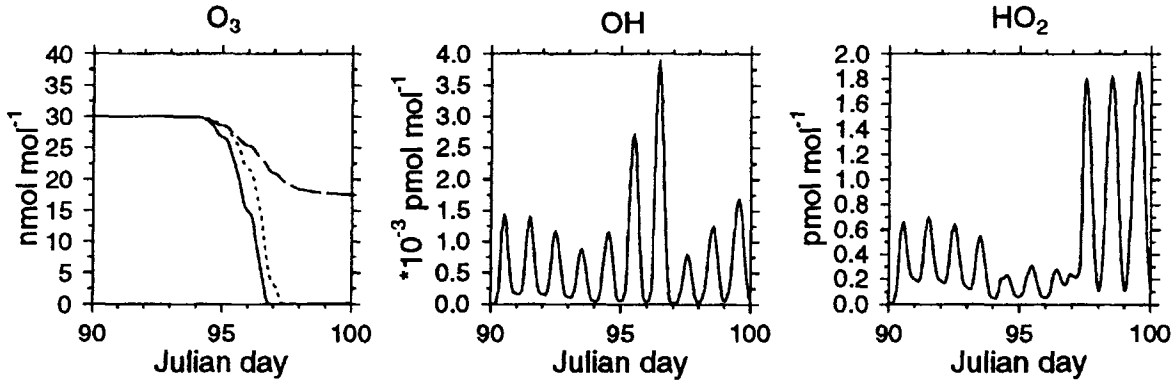

Fig. 1. Gas-phase mixing ratios of O_3, OH, and HO_2 in the base run of the model (solid) and O_3 in sensitivity studies without iodine (dotted) and without R'Br recycling (dashed). See text for details. A mixing ratio of 1 pmol/mol is equivalent to a concentration of about 3×10^7 molecules/cm^3.

this cycle on ozone:

$$\begin{aligned} &Br + O_3 \rightarrow BrO + O_2 \\ &BrO \xrightarrow{h\nu} Br + O \\ &O + O_2 \rightarrow O_3 \\ &\text{null cycle} \end{aligned}.$$

If, however, BrO is converted back to Br without producing oxygen atoms, there is a net loss of ozone:

$$\begin{aligned} &2(Br + O_3 \rightarrow BrO + O_2) \\ &BrO + BrO \rightarrow 2Br + O_2 \\ &\text{cycle a: } 2O_3 \rightarrow 3O_2 \end{aligned}.$$

It should be noted here that another product of the BrO self reaction is Br_2. This is included in the model. As Br_2 is quickly photolyzed, this channel likewise leads to destruction of ozone.

Another cycle that leads to the destruction of ozone involves the reaction of BrO with HO_2:

$$\begin{aligned} &Br + O_3 \rightarrow BrO + O_2 \\ &BrO + HO_2 \rightarrow HOBr + O_2 \\ &HOBr \xrightarrow{h\nu} Br + OH \\ &OH + CO \xrightarrow{O_2} HO_2 + CO_2 \\ &\text{cycle b: } O_3 + CO \rightarrow O_2 + CO_2 \end{aligned}$$

The importance of this bromine-catalyzed ozone depletion was originally suggested by Barrie et al. (1988) and is now generally accepted. Reactions of iodine are similar to those of bromine. Inclusion of iodine chemistry adds another ozone-destruction cycle:

$$\begin{aligned} &Br + O_3 \rightarrow BrO + O_2 \\ &I + O_3 \rightarrow IO + O_2 \\ &BrO + IO \rightarrow Br + I + O_2 \\ &\text{cycle c: } 2O_3 \rightarrow 3O_2 \end{aligned}.$$

Ozone destruction under the conditions of our model run was almost completely due to cycles a–c. The rates of the key reactions of these cycles are plotted in Fig. 2.

To test the importance of the iodine containing cycle c we have performed a sensitivity study without any iodine species. Fig. 1 (dotted line) shows that the ozone mixing ratios during the depletion are about 5 nmol/mol higher than in the base run in which iodine had been included.

Critical reactions in the bromine budget are the additions of Br atoms to ethene and ethyne. We found that the nature of the reaction products is important for the budget of bromine. In the base run, we assume that the R'Br produced undergoes further reactions in which Br is regenerated. The steady-state mixing ratio of R'Br reaches about 10 pmol/mol during the ozone depletion event. In a sensitivity study, we assume that R'Br is a stable end product and thus the bromine atom in it is irreversibly lost. This led to lower bromine atom concentrations and an incomplete ozone destruction (dashed line in Fig. 1) even though the halogen emission rates were the same as in the base run. Changing the parameterization of these reactions in the model thus affects the critical emission source strength needed to explain the ozone deple-

tion. More data about the kinetics and the product distributions of the addition of Br to C_2H_4 and C_2H_2 are needed in order to investigate the bromine budget more exactly.

3.2. *Gas-phas halogen partitioning*

In Fig. 3, gas-phase mixing ratios of some halogen species are presented. From JD 90 until the end of JD 93, the only bromine source is the photolysis of $CHBr_3$ (and to a much smaller extent oxidation of CH_3Br). HOBr is the most abundant bromine species. However, its mixing ratio does not exceed 1 pmol/mol (Fig. 3b). During the ozone depletion phase (JD 94 until JD 97), BrO mixing ratios reach about 30 pmol/mol, which is in good agreement with some results from field measurements (Hausmann & Platt, 1994). Due to their rapid recycling on the sulfate aerosol, HOBr and HBr mixing ratios are significantly smaller than BrO, and reach maximum values of 13 and 12 pmol/mol, respectively. At night the formation of HOBr is decreased because of the lower HO_2 concentration, and the predominant bromine species is BrCl.

The gas-phase chlorine partitioning is shown in Fig. 3a. Chlorine atoms formed by photolysis of Cl_2 rapidly react with hydrocarbons. HCl mixing ratios increase to several hundred pmol/mol. However, this value could be too high since the current model version does not consider scavenging of HCl by alkaline sea-salt aerosol particles. Because of the presence of reactive hydrocarbons, the Cl concentration does not exceed 1.3×10^4 cm^{-3}. The maximum ClO mixing ratio of 1.4 pmol/mol is reached during the first depletion day (JD 94).

The mixing ratios of iodine species are shown in Fig. 3c. During the first day of ozone depletion, IO is the most abundant inorganic iodine species and reaches approximately 1 pmol/mol. This is close to the observations by Unold et al. (1996), who found that IO could have reached up to 0.5 pmol/mol. The I/IO ratio is much larger than Br/BrO or Cl/ClO, because of the larger absorption cross section of IO and the very low reactivity of I atoms towards hydrocarbons. Due to the fast photolysis of HOI, its mixing ratio is only about 0.2 pmol/mol. Consequently the reactions of HOI with Cl^- and Br^- are only a minor importance for recycling of bromine or chlorine. When O_3 is depleted the I atom mixing ratio increases to about 4 pmol/mol. This value could be too high since the current model neglects scavenging of I atoms by aerosol particles.

3.3. *Aqueous-phase chemistry*

As shown above, catalytic cycles involving gas-phase Br atoms can efficiently destroy ozone. Reactions of Br with aldehydes terminate the chain and form highly soluble HBr which is scavenged by aerosol particles. To compensate for this heterogeneous loss, it is necessary to transform aqueous HBr (and HOBr) into more active species which can re-enter the ozone destruction chain in the gas phase. This is accomplished by reactions (2) and (3), as described above. The distribution of bromine species between the phases is shown in Fig. 4a. During the ozone depletion event, most

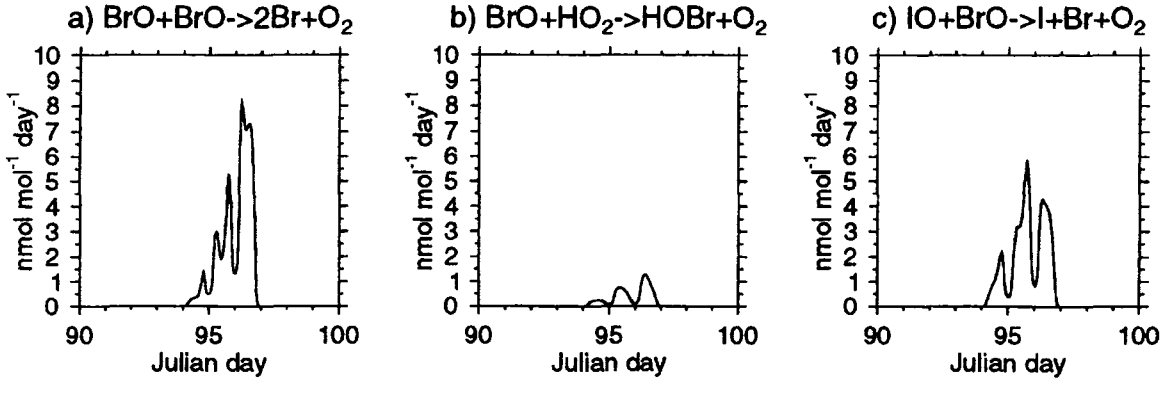

Fig. 2. Rates of the key reactions in cycles a, b, and c responsible for the destruction of ozone in the base run of the model.

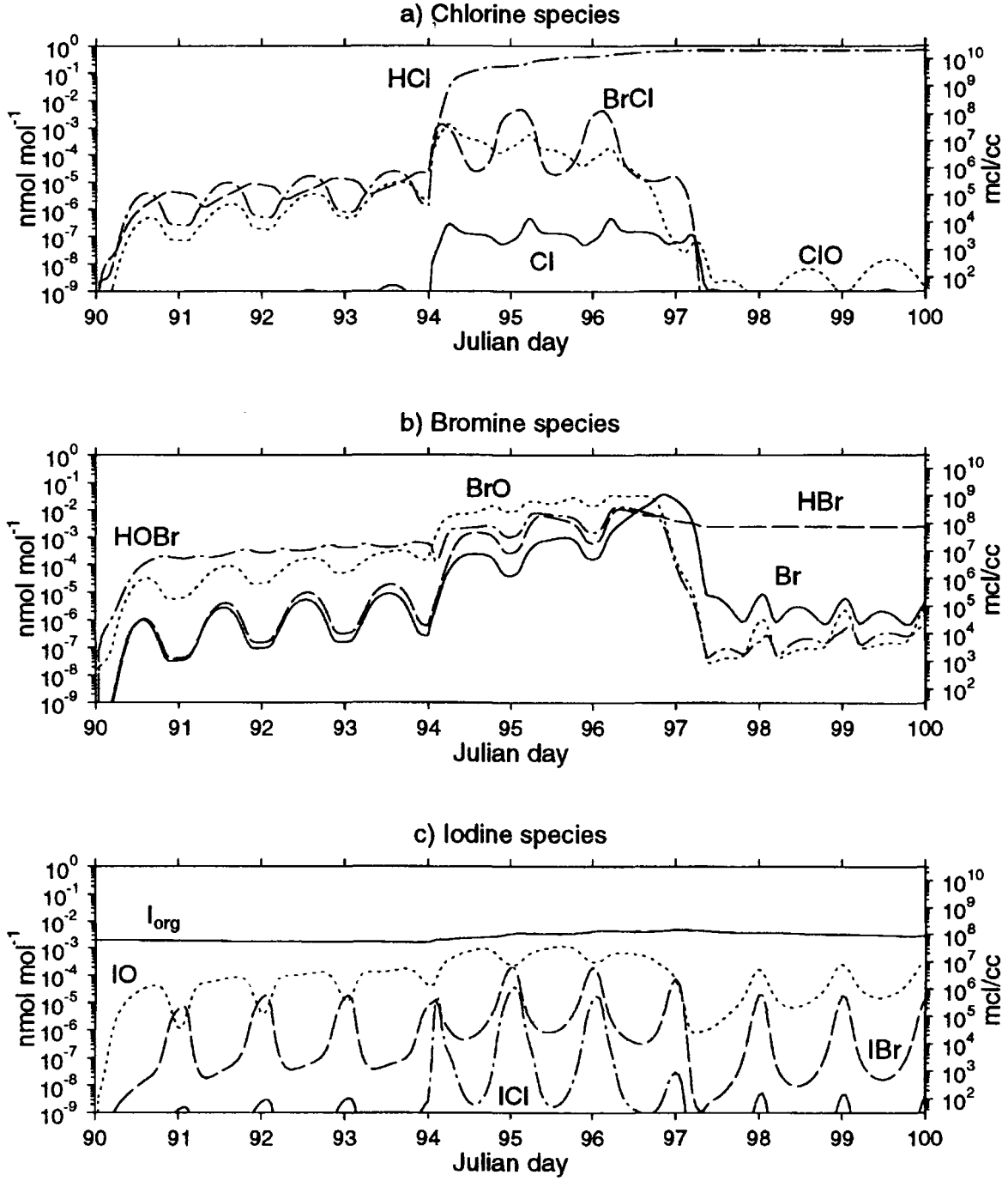

Fig. 3. Gas-phase distribution of some chlorine (a), bromine (b), and iodine (c) species; $I_{org} \equiv CH_3I + C_3H_7I + CH_2ClI + 2CH_2I_2$.

of the HBr that is scavenged from the gas phase quickly reacts with HOBr, and the resulting Br_2 volatilizes. Thus, most of the bromine is in the gas phase. However, when ozone is depleted, the gas-phase production of HOBr stops since the reaction sequence

$$Br \xrightarrow{O_3} BrO \xrightarrow{HO_2} HOBr$$

depends on the availability of ozone. Without

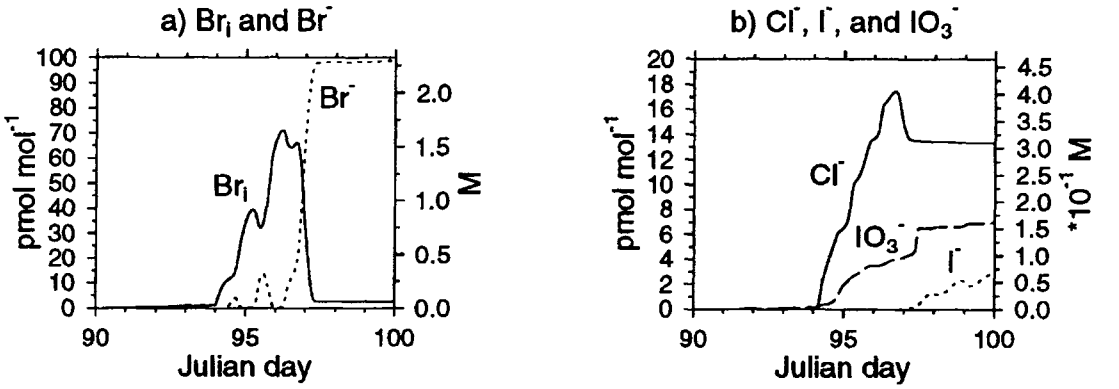

Fig. 4. (a) Distribution of bromine species between the phases. Br_i is the sum of inorganic bromine species in the gas phase. (b) Chlorine and iodine species in the aqueous phase.

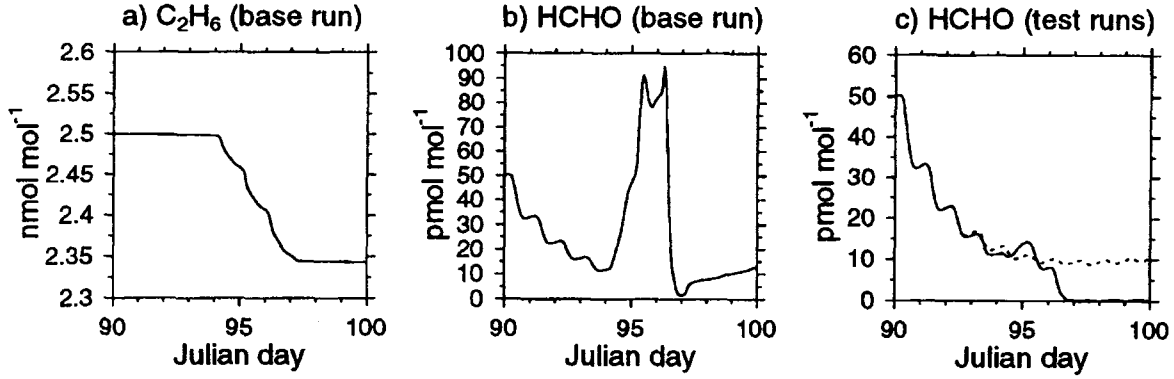

Fig. 5. Gas-phase mixing ratios of (a) C_2H_6 and (b) HCHO in the base run. In (c), the mixing ratio of HCHO in sensitivity studies without chlorine (solid) and without any halogen emissions (dotted) is shown. See text for details. A mixing ratio of 1 pmol/mol is equivalent to a concentration of about 3×10^7 molecules/cm^3.

HOBr being supplied from the gas phase, there is no way to re-activate Br^-. It now accumulates in the aerosol particles, and bromine species disappear from the gas phase except for some remaining HBr.

In Fig. 4b, the aqueous-phase concentrations of Cl^-, IO_3^-, and I^- are shown. During the ozone depletion event, the chloride content of the aerosol gradually increases. However, most of the HCl which has been scavenged from the gas phase is recycled via reaction with HOBr (3). The model also describes the formation of particulate iodine, which is mainly iodate formed via reaction (16). Only in the absence of hypohalous acids, i.e., after all O_3 has been depleted, iodide accumulates in the aerosol. Note that in the model, there is no loss process for the sulfate aerosol, and therefore rather high concentrations of particulate iodine are reached.

3.4. The chemistry of NMHCs and HCHO during ozone depletion events

Initial concentrations of NMHCs were set to values typically observed in the arctic spring (Table 1). The emission rate of chlorine was chosen to match the observed decay of alkanes during ozone depletion events. The mixing ratio of C_2H_6 is shown as an example in Fig. 5a. By considering the additional attack by Br atoms, the decay of C_2H_4 and C_2H_2 can also be reproduced well.

Other than the NMHCs, which decrease during ozone depletion events, measurements showed that HCHO increases in that period (De Serves, 1994). This is an apparent contradiction to the fact that HCHO is destroyed by reactions with halogen atoms. However, chlorine chemistry also introduces a large source of HCHO: The reactions of alkanes with Cl produce peroxy radicals which

in turn produce HCHO via reactions (8) and (11). The modeled mixing ratio of HCHO increases to about 100 pmol/mol during the depletion of O_3, as shown in Fig. 5b. Our results show a strong positive correlation between halogen atoms and HCHO. However, our model is unable to reproduce mixing ratios as high as 600 pmol/mol as observed by De Serves (1994). In a very recent paper, Shepson et al. (1996) came to a similar conclusion about the discrepancy between modeled and observed concentrations of HCHO.

It is interesting to note that the modeled production of peroxy radicals (and thus that of HCHO) does not change much when the initial hydrocarbon concentrations are increased. This can be visualized by a very simplified steady-state calculation. The production of peroxy radicals RO_2 from hydrocarbons RH and Cl is given by:

$$\frac{d[RO_2]}{dt} = k_{RH} \times [RH] \times [Cl], \quad (17)$$

with k_{RH} = rate constant for RH + Cl. The steady-state concentration $[Cl]_{ss}$ is:

$$\frac{d[Cl]}{dt} = P - k_{RH} \times [RH] \times [Cl] - k_1 \times [Cl] = 0 \quad (18)$$

$$\Rightarrow [Cl]_{ss} = \frac{P}{k_{RH} \times [RH] + k_1}, \quad (19)$$

with P = production rate of Cl, and k_1 = 1st-order rate constant for loss of Cl due to reactions other than with hydrocarbons. Inserting $(Cl)_{ss}$ into eq. (17) yields:

$$\frac{d[RO_2]}{dt} = P \times \frac{k_{RH} \times [RH]}{k_{RH} \times [RH] + k_1} \approx P. \quad (20)$$

Thus, as long as Cl mainly reacts with hydrocarbons (i.e. $k_1 \ll k_{RH} \times (RH)$], the production of RO_2 is independent of the hydrocarbon concentration.

In further sensitivity studies, we look at the effect of bromine on HCHO. Fig. 5c shows model runs without any halogen emissions (dotted line) and with emissions of bromine only (solid line). Without halogens present, HCHO decreases from the initial value of 50 pmol/mol to a steady-state value around 10 pmol/mol. In the run in which bromine is emitted on JD 94, an anticorrelation between Br and HCHO could be expected from the fast reaction Br + HCHO. However, the HCHO mixing ratios are initially not very different form the run without halogens. The complete destruction of HCHO does not occur until ozone has been depleted, which is around JD 97. To understand this phenomenon, we consider the role of HOBr which leads to another source of HCHO. HOBr is produced during the ozone depletion in cycle b. Its photolysis increases the concentration of OH. The reactions of OH with alkanes produce peroxy radicals which in turn produce HCHO as shown above. This channel compensates for the loss of HCHO via reaction with Br atoms.

4. Conclusions

Using a photochemical box model to describe ozone loss in the springtime Arctic boundary layer we find that:

- a source strength of about 17 pmol mol^{-1} day^{-1} bromine is necessary to explain BrO levels of up to 30 pmol/mol and complete ozone destruction within three days;
- a critical parameter in the determination of the source strength is the quantification of the bromine sink via reaction with ethene or ethyne and possible regeneration of Br from the reaction products;
- assuming a source strength of about 3 pmol mol^{-1} day^{-1} or organic iodine, approximately 20% of the ozone is depleted by iodine chemistry; the major iodine-containing gas-phase reaction that destroys ozone is the reaction of BrO with IO.
- after the depletion of ozone, gas-phase bromine species are converted into HBr and scavenged by the aerosol particles; particulate iodine is mainly IO_3^-; only after the depletion of O_3, iodide can accumulate in the aerosol;
- due to simultaneous occurrence of chlorine and bromine during ozone depletion events, Br and HCHO are positively correlated; however, concentrations as high as those observed by De Serves (1994) cannot be reproduced with the model; even in the absence of Cl, HCHO is not destroyed by Br until the ozone depletion is complete.

5. Acknowledgements

We would like to thank T. Tang, J. C. McConnell, and C. Brühl for calculating

photolysis rates. We are grateful to C. Roehl for providing us with UV spectra of several iodine compounds prior to publication. We also thank P. Ariya for help in adjusting the model to conditions as encountered during the polar sunrise campaigns 1994 and 1995. This work was funded in part by British Gas.

REFERENCES

Barnes, I., Bastian, V., Becker, K. H., Overath, R. & Tong, Z. 1989. Rate constants for the reactions of Br atoms with a series of alkanes, alkenes, and alkynes in the presence of O_2. *Int. J. Chem. Kinetics*, **21**, 499–517.

Barrie, L. A., Bottenheim, J. W., Schnell, R. C., Crutzen, P. J. & Rasmussen, R. A. 1988. Ozone destruction and photochemical reactions at polar sunrise in the lower Arctic atmosphere. *Nature*, **334**, 138–141.

Barrie, L. A., Staebler, R., Toom, D., Georgi, B., den Hartog, G., Landsberger, S. & Wu, D. 1994. Arctic aerosol size-segregated chemical observations in relation to ozone depletion during Polar Sunrise Experiment 1992. *J. Geophys. Res.* **99D**, 25439–25451.

Beckwith, R. C., Wang, T. X. & Margerum, D. W. 1996. Equilibrium and kinetics of bromine hydrolysis. *Inorg. Chem.* **35**, 995–1000.

Berg, W. W., Sperry, P. D., Rahn, K. A. & Gladney, E. S. 1983. Atmospheric bromine in the arctic. *J. Geophys. Res.* **88C**, 6719–6736.

Brühl, C. & Crutzen, P. J. 1989. On the disproportionate role of tropospheric ozone as a filter against solar UV-B radiation. *Geophys. Res. Lett.* **16**, 703–706.

Chameides, W. L. & Davis, D. D. 1980. Iodine: Its possible role in tropospheric photochemistry. *J. Geophys. Res.* **85C**, 7383–7398.

Chatfield, R. B. & Crutzen, P. J. 1990. Are there interactions of iodine and sulfur species in marine air photochemistry? *J. Geophys. Res.* **95D**, 22319–22341.

Davis, D., Crawford, J., Liu, S., McKeen, S., Bandy, A., Thornton, D., Rowland, F. & Blake, D. 1996. Potential impact of iodine on tropospheric levels of ozone and other critical oxidants. *J. Geophys. Res.* **101D**, 2135–2147.

De Serves, C. 1994. Gas phase formaldehyde and peroxide measurements in the arctic atmosphere. *J. Geophys. Res.* **99D**, 25391–25398.

Eigen, M. & Kustin, K. 1962. The kinetics of halogen hydrolysis. *J. Am. Chem. Soc.* **84**, 1355–1361.

Fan, S.-M. & Jacob D. J. 1992. Surface ozone depletion in Arctic spring sustained by bromine reactions on aerosols. *Nature* **359**, 522–524.

Hausmann, M. & Platt, U. 1994. Spectroscopic measurement of bromine oxide and ozone in the high Arctic during polar sunrise experiment 1992. *J. Geophys. Res.* **99D**, 25399–25413.

Heidt, L. E., Krasnec, J. P., Lueb, R. A., Pollock, W. H., Henry, B. E. & Crutzen, P. J. 1980. Latitudinal distributions of CO and CH_4 over the Pacific. *J. Geophys. Res.* **85C**, 7329–7336.

Henderson, G. S., McConnell, J. C., Templeton, E. M. J. & Evans, W. F. J. 1987. A numerical model for one-dimensional simulation of stratospheric chemistry. *Atmos. Ocean* **25**, 427–459.

Jenkin, M. E. 1992. The photochemistry of iodine-containing compounds in the marine boundary layer. Tech. Rep. AEA-EE-0405, United Kingdom Atomic Energy Authority, Harwell Laboratory, Oxon, OX11 ORA, UK.

Jobson, B. T., Niki, H., Yokouchi, Y., Bottenhein, J., Hopper, F. & Leaitch, R. 1994. Measurements of C_2–C_6 hydrocarbons during the polar sunrise 92 experiment: Evidence for Cl-atom and Br-atom chemistry. *J. Geophys. Res.* **99D**, 25355–25368.

Klick, S. & Abrahamson, K. 1992. Biogenic volatile iodated hydrocarbons in the ocean. *J. Geophys. Res.* **97C**, 12683–12687.

Kumar, K. & Margerum, D. W. 1987. Kinetics and mechanism of general-acid-assisted oxidation of bromide by hypochlorite and hypochlorous acid. *Inorg. Chem.* **26**, 2706–2711.

Laszlo, B., Kurylo, M. J. & Huie, R. E. 1995. Absorption cross sections, kinetics of formation, and self-reaction of the IO radical produced via the laser photolysis of $N_2O/I_2/N_2$ mixtures. *J. Phys. Chem.* **99**, 11710–11707.

Laszlo, B., Huie, R. E., Kurylo, M. J. & Miziolek, A. W. 1996. Kinetics studies of the reactions of BrO and IO radicals. *J. Geophys. Res*, in press.

Moore, R. M. & Tokarczyk, R. 1992. Chloro-iodomethane in N. Atlantic waters. A potentially significant source of atmospheric iodine. *Geophys. Res. Lett.* **19**, 1779–17892.

Muthuramu, K., Shepson, P. B., Bottenheim, J. W., Jobson, B. T., Niki, H. & Anlauf, K. G. 1994. Relationships between organic nitrates and surface ozone destruction during Polar Sunrise Experiment 1992. *J. Geophys. Res.* **99D**, 25369–25378.

Nagy, J. C., Kumar, K. & Margerum, D. W. 1988. Nonmetal redox kinetics: Oxidation of iodide by hypochlorous acid and by nitrogen trichloride measured by the pulsed-accelerated-flow method. *Inorg. Chem.* **27**, 2773–2780.

Oltmans, S. J. & Komhyr, W. D. 1986. Surface ozone distributions and variations from 1973–1984 measurements at the NOAA geophysical monitoring for climatic change baseline observatories. *J. Geophys. Res.* **91D**, 5229–5236.

Pruppacher, H. R. & Klett, J. D. 1978. *Microphysics of Cloud and Precipitation.* D. Reidel, London.

Roehl, C. M., Burkholder, J. B., Moortgat, G. K., Rav-

ishankara, A. R. & Crutzen, P. J. 1997. The temperature dependence of the UV absorption cross sections and the atmospheric implications of several alkyl iodides. *J. Geophys. Res.* **102D**, 12819–12829.

Sander, R. & Crutzen, P. J. 1996. Model study indicating halogen activation and ozone destruction in polluted air masses transported to the sea. *J. Geophys. Res.* **101D**, 9121–9138.

Schall, C. & Heumann, K. G. 1993. GC determination of volatile organoiodine and organobromine compounds in Arctic seawater and air samples. *Fresenius J. Anal. Chem.* **346**, 717–722.

Seery, D. J. & Britton, D. 1964. The continuous absorption spectra of chlorine, bromine, bromine chloride, iodine chloride, and iodine bromide. *J. Phys. Chem.* **68**, 2263–2266.

Shepson, P. B., Sirju, A.-P., Hopper, J. F., Barrie, L. A., Young, V., Niki, H. & Dryfhout, H. 1996. Sources and sinks of carbonyl compounds in the Arctic ocean boundary layer: Polar ice flow experiment. *J. Goephys. Res.* **101D**, 21081–21089.

Staebler, R. M., den Hartog, G., Georgi, B. & Düsterdiek, T., 1994. Aerosol size distributions in Arctic haze during the Polar Sunrise experiment 1992. *J. Geophys. Res.* **99D**, 25429–25437.

Stull, R. B. 1988. *An introduction to boundary-layer meteorology*. Kluwer Academic Publishers, Dordrecht, The Netherlands.

Tellinghuisen, J. 1973. Resolution of the visible-infrared absorption spectrum, I_2 into three contribution transitions. *J. Chem. Phys.* **58**, 2821–2834.

Troy, R. C. & Margerum, D. W. 1991. Non-metal redox kinetics: Hypobromite and hypobromous acid reactions with iodide and with sulfite and the hydrolysis of bromosulfate. *Inorg. Chem.* **30**, 3538–3543.

Troy, R. C., Kelley, M. D., Nagy, J. C. & Margerum, D. W. 1991. Non-metal redox kinetics: Iodine monobromide reaction with iodide ion and the hydrolysis of IBr. *Inorg. Chem.* **30**, 4838–4845.

Turnipseed, A. A., Gilles, M. K., Burkholder, J. B. & Ravishankara, A. R. 1995. Iodine chemistry in the stratosphere: Kinetics of the IO + ClO and IO + BrO reactions. *Eos, Trans. AGU* (abstr. suppl) **76/46**, F116.

Unold, W., Lorenzen-Schmidt, H., Stutz, J., Trost, B. & Platt, U. 1996. Measurements of halogen oxides in the Arctic boundary layer during spring '95. *Ann. Geophys.* **14** (suppl. II) C606.

Vogt, R., Crutzen, P. J. & Sander, R. 1996. A mechanism for halogen release from sea-salt aerosol in the remote marine boundary layer. *Nature*, **382**, 327–330.

Wang, T. X. & Margerum, D. W. 1994. Kinetics of reversible chlorine hydrolysis: Temperature dependence and general-acid/base-assisted mechanisms. *Inorg. Chem.* **33**, 1050–1055.

Wang, T. X., Kelley, M. D., Cooper, J. N., Beckwith, R. C. & Margerum, D. W. 1994. Equilibrium, kinetic and UV-spectral characteristics of aqueous bromine chloride, bromine, and chlorine species. *Inorg. Chem.* **33**, 5872–5878.

Wang, Y. L., Nagy, J. C. & Margerum, D. W. 1989. Kinetics of hydrolysis of iodine monochloride measured by the pulsed-accelerated-flow method. *J. Am. Chem. Soc.* **111**, 784 38–7844.

Wayne, R. P., Poulet, G., Biggs, P., Burrows, J. P., Cox, R. A., Crutzen, P. J., Hayman, G. D., Jenkin, M. E., Le Bras, G., Moortgat, G. K., Platt, U. & Schindler, R. N. 1995. Halogen oxides: Radicals, sources and reservoirs in the laboratory and in the atmosphere. *Atmos. Environ.* **29**, 2677–2881.

Worthy, D. E. J., Trivett, N. B. A., Hopper, J. F. & Bottenheim, J. W. 1994. Analysis of long-range transport events at Alert, Northwest Territories, during the Polar Sunrise Experiment. *J. Geophys. Res.* **99D**, 25329–25344.

Yarwood, G., Niki, H. & Maker, P. D. 1991. Kinetic and IR spectroscopic studies of formyl bromide (HCOBr) formed via the reaction $HCO + Br_2 \rightarrow HCOBr + Br$. *J. Phys. Chem.* **95**, 4773–4777.

Yarwood, G., Peng, N. & Niki, H. 1992. FTIR spectroscopic study of the Cl- and Br-atom initiated oxidation of ethene. *Int. J. Chem. Kinetics* **24**, 369–383.

Yokouchi, Y., Akimoto, H., Barrie, L. A., Bottenheim, J. W., Anlauf, K. G. & Jobson, B. T. 1994. Serial gas chromatographic/mass spectrometric measurements of some volatile organic compounds in the arctic atmosphere during the 1992 Polar Sunrise Experiment. *J. Geophys. Res.* **99D**, 25379–25389.